

Synthesis and Evaluation of Doxorubicin-Loaded Gold Nanoparticles for Tumor-Targeted Drug Delivery

Yongle Du, Long Xia, Ami Jo, Richey M. Davis, Philippe Bissel, Marion Ehrich, and David George Ian Kingston

Bioconjugate Chem., **Just Accepted Manuscript** • DOI: 10.1021/acs.bioconjchem.7b00756 • Publication Date (Web): 20 Dec 2017

Downloaded from <http://pubs.acs.org> on December 21, 2017

Just Accepted

“Just Accepted” manuscripts have been peer-reviewed and accepted for publication. They are posted online prior to technical editing, formatting for publication and author proofing. The American Chemical Society provides “Just Accepted” as a free service to the research community to expedite the dissemination of scientific material as soon as possible after acceptance. “Just Accepted” manuscripts appear in full in PDF format accompanied by an HTML abstract. “Just Accepted” manuscripts have been fully peer reviewed, but should not be considered the official version of record. They are accessible to all readers and citable by the Digital Object Identifier (DOI®). “Just Accepted” is an optional service offered to authors. Therefore, the “Just Accepted” Web site may not include all articles that will be published in the journal. After a manuscript is technically edited and formatted, it will be removed from the “Just Accepted” Web site and published as an ASAP article. Note that technical editing may introduce minor changes to the manuscript text and/or graphics which could affect content, and all legal disclaimers and ethical guidelines that apply to the journal pertain. ACS cannot be held responsible for errors or consequences arising from the use of information contained in these “Just Accepted” manuscripts.

Synthesis and Evaluation of Doxorubicin-Loaded Gold Nanoparticles for Tumor-Targeted Drug Delivery

Yongle Du,[†] Long Xia,[†] Ami Jo,[‡] Richey M. Davis,[‡] Philippe Bissel,[§] Marion F. Ehrich,[§] and David G. I. Kingston^{*†}

[†]Department of Chemistry and the Virginia Tech Center for Drug Discovery, Virginia Tech, Blacksburg, Virginia 24061, United States

[‡]Department of Chemical Engineering and the Virginia Tech Center for Drug Discovery, Virginia Tech, Blacksburg, Virginia 24061, United States

[§]Virginia-Maryland College of Veterinary Medicine and the Virginia Tech Center for Drug Discovery, Virginia Tech, Blacksburg, Virginia 24061, United States

Supporting Information

ABSTRACT: Doxorubicin is an effective and widely used cancer chemotherapeutic agent, but its application is greatly compromised by its cumulative dose-dependent side effect of cardiotoxicity. A gold nanoparticle-based drug delivery system has been designed to overcome this limitation. Five novel thiolated doxorubicin analogs were synthesized and their biological activities evaluated. Two of these analogs and PEG stabilizing ligands were then conjugated to gold nanoparticles, and the resulting Au-Dox constructs were evaluated. The results show that release of native drug can be achieved by the action of reducing agents such as glutathione or under acidic conditions, but that reductive drug release gave the cleanest drug release. Gold

nanoparticles (Au-Dox) were prepared with different loadings of PEG and doxorubicin, and one formulation was evaluated for mammalian stability and toxicity. Plasma levels of doxorubicin in mice treated with Au-Dox were significantly lower than in mice treated with the same amount of doxorubicin, indicating that the construct is stable under physiological conditions. Treatment of mice with Au-Dox gave no histopathologically observable differences from mice treated with saline, while mice treated with an equivalent dose of doxorubicin showed significant histopathologically observable lesions.

■ INTRODUCTION

The anthracycline antibiotic doxorubicin (**1**, Figure 1) was discovered in the late 1960's as a minor component of the fermentation broth used to produce its analog daunorubicin (**2**).¹ Daunorubicin itself was discovered in the 1950's from a strain of *Streptomyces peucetius* isolated from a soil sample collected near the Adriatic Sea;² it had good bioactivity against mouse tumors, and was eventually marketed for treatment of leukemia.³ Doxorubicin was identified as a hydroxylated analog of daunorubicin and was initially named adriamycin after the source of the original soil sample, but was later renamed doxorubicin by the World Health Organization.

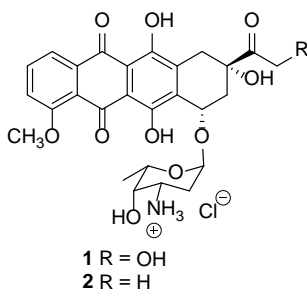


Figure 1. Doxorubicin (**1**) and daunorubicin (**2**).

1
2
3 Doxorubicin has a wide spectrum of activity and is used today, either alone or in
4
5 combination with other drugs, for the treatment of a variety of cancers, including acute
6
7 leukemias and ovarian and breast cancers. It is one of the most effective cancer
8
9 chemotherapeutic agents available,⁴⁻⁷ and is on the World Health Organization list of essential
10
11 medicines for both adults and children.⁸ Regrettably its use is severely limited by various side
12
13 effects, including myelosuppression, vomiting, diarrhea, and especially life-threatening
14
15 cardiotoxicity.^{9, 10} Two liposomal formulations of doxorubicin have been approved for clinical
16
17 use. Doxil[®], available in the U.S., is a pegylated liposomal formulation of doxorubicin that is
18
19 approved for treatment of Kaposi's sarcoma, ovarian cancer, and multiple myeloma; it is much
20
21 less cardiotoxic than native doxorubicin, but it does have some new side-effects.¹¹ Myocet[®]
22
23 (liposome encapsulated doxorubicin citrate), available in the U.K., also is less cardiotoxic than
24
25 doxorubicin and can be better tolerated by patients, while having an equivalent therapeutic
26
27 efficacy.¹² While these formulations of doxorubicin are an improvement over the native drug,
28
29 there is still room for further improvement, and it is a measure of doxorubicin's clinical
30
31 effectiveness that it is so widely used in spite of its very significant side effects. Clearly however
32
33 a selective targeted drug delivery method would offer the opportunity to make doxorubicin an
34
35 even better option for cancer treatment.

36
37
38 The basic idea of targeting cancer chemotherapeutic agents is well known, and several
39
40 approaches to targeting doxorubicin have been published. These include targeted delivery to
41
42 hepatocarcinoma cells by laponite nanodiscs,¹³ the use of magnetoliposomes,¹⁴ and the use of
43
44 doxorubicin-loaded poly(lactic-co-glycolic acid) hollow microcapsules.¹⁵ The nanoparticle
45
46 approach to drug delivery is attractive, since the enhanced permeability and retention effect
47
48 assures a measure of selectivity,¹⁶ although the magnitude of this effect has been questioned by a
49
50
51
52
53
54
55
56
57
58
59
60

1
2
3 meta-analysis which showed that only 0.7% of the administered dose of nanoparticle drugs is
4 delivered to solid tumors.¹⁷ Even this relatively low number is however higher than that of naked
5 drug molecules,¹⁸ and in the particular case of doxorubicin even this low delivery efficiency
6 could be significant if the remaining drug never reached the heart.
7
8
9
10

11
12 The use of gold nanoparticles (AuNP) for drug delivery is particularly attractive since
13 they can be generated in a range of sizes and can readily be functionalized with a variety of
14 ligands,¹⁹ and numerous studies have been made of AuNPs conjugated with doxorubicin. In
15 some cases protonated doxorubicin was absorbed directly onto the surface of negatively charged
16 AuNP under acidic conditions,²⁰ and a one-pot synthesis of doxorubicin-loaded AuNP was
17 achieved in the presence of oxygen to generate radicals.²¹ Several studies used various polymers
18 to link doxorubicin to AuNP. Thus doxorubicin was loaded onto anionic polyaspartic acid AuNP
19 by ionic complexation,²² or it was bound to DNA which was itself bound to the AuNP.²³ Another
20 study used DNA-caged AuNP that allowed T7 exonuclease and pH responsive controlled release
21 of doxorubicin.²⁴ A study of doxorubicin-loaded PEG-AuNPs and their further antibody
22 targeting showed that toxicity was reduced and therapeutic efficacy increased for the antibody
23 targeted system.²⁵ On the other hand, a study of PEGylated gold nanoparticles with doxorubicin
24 attached by covalent peptide or pH-active hydrazone linkers revealed that gold nanostructures
25 modified with doxorubicin were more toxic to A549 and HeLa cells than free doxorubicin.²⁶ The
26 use of folate-modified pegylated AuNP to conjugate doxorubicin gave a drug system that
27 showed a much higher cytotoxicity than that of free doxorubicin, as well as an increased water-
28 solubility.²⁷ Another study of folic acid-coated AuNP gave a construct with enhanced drug
29 accumulation and retention in multidrug resistant hepG2-R cancer cells compared with free
30 doxorubicin.²⁸ Grafting a thiolated doxorubicin onto AuNPs via a cleavable disulfide linkage
31
32
33
34
35
36
37
38
39
40
41
42
43
44
45
46
47
48
49
50
51
52
53
54
55
56
57
58
59
60

(Au-PEG-SS-DOX) improved drug uptake as compared with native doxorubicin, although the drug released was a doxorubicin derivative.²⁹ A study of a formulation with a pH-sensitive hydrazone bond as linker between doxorubicin and pegylated AuNP showed greatly enhanced solubility and an excellent pH response profile of drug release for the drug construct.³⁰ A variation of this approach grafted doxorubicin by a cleavable hydrazone linker onto the hydrophobic inner shell of a folate-conjugated poly(L-aspartate-doxorubicin)-*b*-poly(ethylene glycol) copolymer to give a drug construct that released doxorubicin readily at pH 5.3.³¹ Ultrasmall gold-doxorubicin conjugates were found to target apoptosis-resistant cancer cells.³² The use of AuNPs for targeted drug delivery¹⁹ has been reviewed, as has the use of iron and gold nanoparticles for doxorubicin delivery,^{19, 33} and the cytotoxicity of AuNPs has recently been evaluated, with the finding that PEG-coated nanospheres, nanorods, and nanostars show low cytotoxicity to U87 cells and fibroblasts.³⁴

The use of AuNPs conjugated with the cytokine tumor necrosis factor (TNF) is a particularly powerful approach to drug targeting, since TNF not only targets the nanoparticle to tumors but also reduces the interstitial fluid pressure, allowing for enhanced uptake of the chemotherapeutic payload.³⁵ In the present study we investigated the conjugation of doxorubicin to AuNPs in preparation for future studies to add TNF to the drug construct.

■ RESULTS

Design and Synthesis of New Thiolated Doxorubicin Analogs. A key consideration in any approach to drug delivery by AuNPs is whether the drug payload is released from the nanoparticle, and if so how this will occur. Release of the native drug from the nanoparticle is preferable, since it allows the drug to interact with its target unhindered by any linker, and so we

prepared the five doxorubicin analogs **3** – **7** (Figure 2) that were designed to release free doxorubicin in the tumor cell.

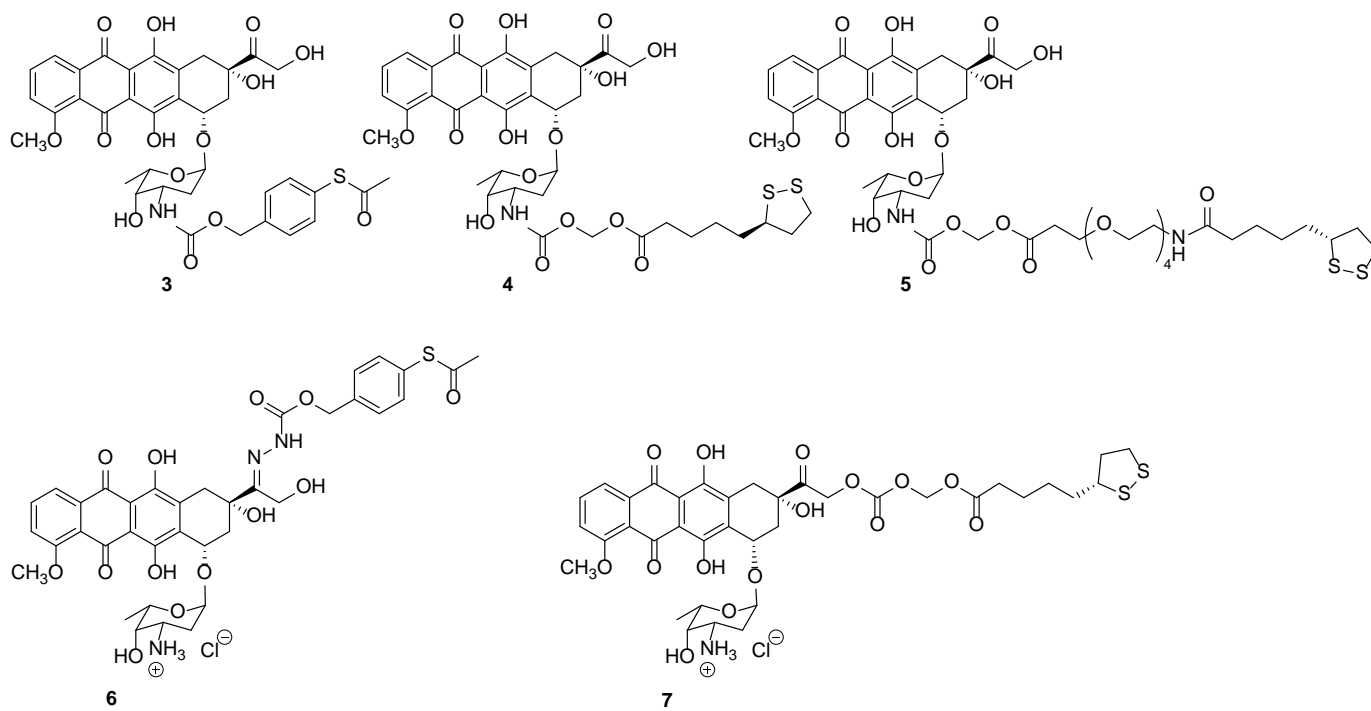


Figure 2. Doxorubicin analogs **3** – **7**.

The 7-*O*-thiobenzyl derivative **3** was designed to undergo reductive cleavage from the AuNP by glutathione in the reducing tumor environment and to release native doxorubicin, as previously described for a similar paclitaxel derivative.³⁵ The proposed mechanism of doxorubicin release is shown in Figure 3, with glutathione displacing analog **3** from the gold surface to give deacetyl **3**, which undergoes self-immolation (arrows) leading to doxorubicin, a thioquinone methide, and carbon dioxide. The thioquinone methide then undergoes hydration to (4-mercaptophenyl)methanol.

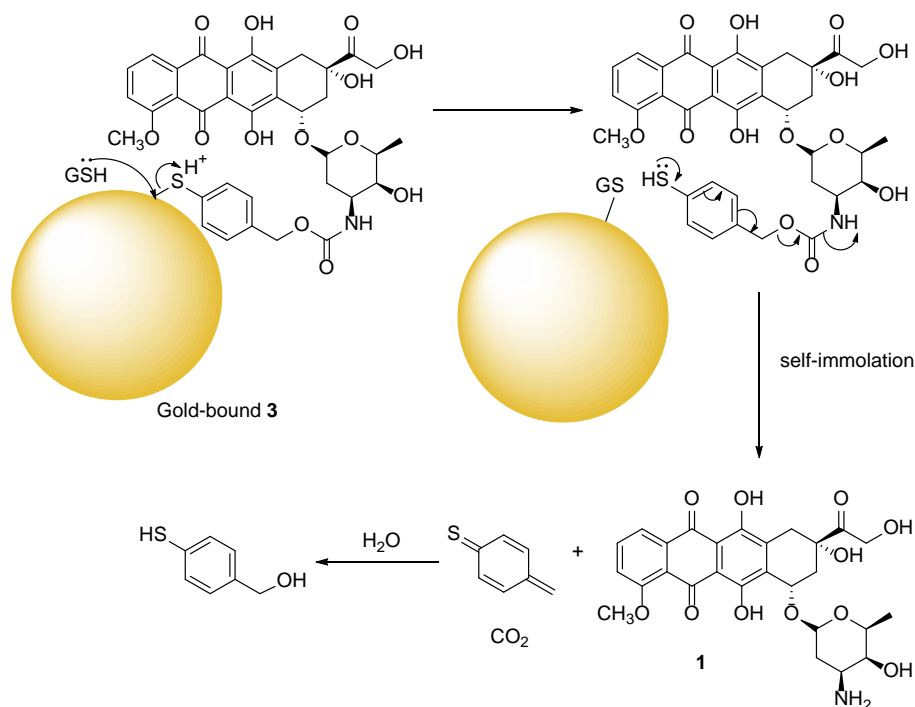
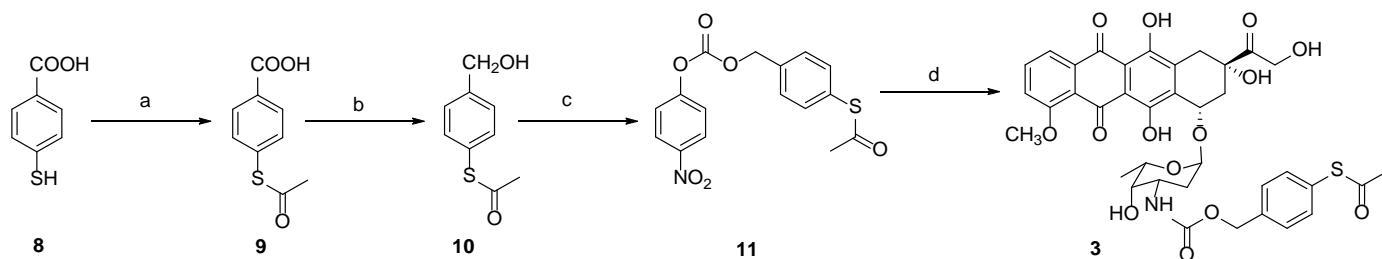


Figure 3. Proposed mechanism of doxorubicin release from gold-bound analog **3** by glutathione (GSH).

The synthesis of analog **3** is shown in Scheme 1. Commercially available 4-mercaptobenzoic acid (**8**) underwent acetylation, reduction and acylation with 4-nitrophenyl chloroformate to obtain compound **11**, which was then reacted directly with doxorubicin hydrochloride (**1**) to give final product **3** in 63% overall yield.

Scheme 1. Synthesis of doxorubicin derivative 3^a



^a(a) Ac₂O, pyridine, CH₂Cl₂, 6 h 0 °C to rt, 98%; (b) Me₂S.BH₃, THF, -10 °C to rt, 4 h, 85%; (c) 4-nitrophenyl chloroformate, pyridine, CH₂Cl₂, 4 h 0 °C to rt, 88%; (d) Et₃N, DMF, **1**, 0 °C to rt, 2 h, 86%;

The syntheses of analogs **4** – **7** are described in the Supporting Information.

Antiproliferative Activities of the Analogs. The antiproliferative activities of the five analogs in the A2780 ovarian cancer cell line were determined (Table 1). All the analogs had similar IC_{50} values to that of doxorubicin, and three of the five (compounds **4**, **6**, and **7**) even had lower values than that of doxorubicin. Although this result is somewhat surprising, it does not affect the selection of analog for linking to gold, since all the analogs were designed to release intact doxorubicin.

Table 1. Antiproliferative Activities of Compounds 3 – 7 Against the A2780 Human Ovarian Cancer Cell Line

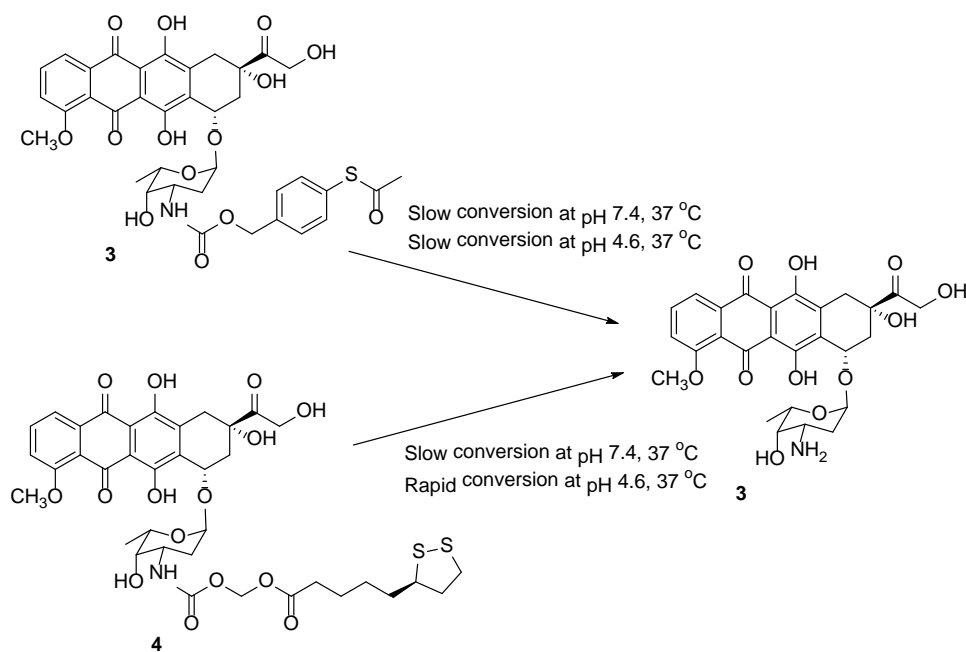
IC ₅₀ values (nM)					
3	4	5	6	7	Doxorubicin (1)
31 ± 5	10 ± 4	28 ± 3	11 ± 5	11 ± 1	26 ± 3

Stability Studies of the Analogs. The HPLC chromatograms of doxorubicin and analogs **3** and **4** (Figures S1 and S2) were used to establish a calibration curve (Figure S3) for analysis of doxorubicin so as to determine the concentration of doxorubicin released from these analogs under various conditions (Scheme 2). Only very slow loss of analog was observed for both **3** and **4** at pH 7.4, with about 90% of the original analog remaining after 3 days at 37 °C (Figure S4). At pH 4.6, however, analog **3** retained its stability, but analog **4** underwent conversion to doxorubicin, with complete loss of **4** after 3 days and formation of doxorubicin (Fig. S5). The half-lives of analog **3** were calculated to be 471 hours at pH 7.4 and 421 hours at pH 4.6; as expected **3** is stable at both neutral and acidic pH values. For analog **4** the corresponding values were 376 and 9.6 hours, consistent with the designed lability of **4** under acidic conditions. Only about 55% of the doxorubicin present in **4** was detected as free doxorubicin, presumably due to slow degradation under the conditions of the experiment. Although doxorubicin only decomposes slowly at pH 4, with less than 10% degradation over 40 hours,³⁶ this stability is

presumed to be due to protonation of the amine group. Since this group is replaced by an amide in **4**, it is possible that acidic decomposition of the anthraquinone moiety proceeds more readily on the unprotonated **4** than on doxorubicin itself.

Analog **3** was selected for detailed examination based on the decomposition observed for **4** under acidic conditions and on the fact that analogs **5** – **7** also require acidic conditions for drug release.

Scheme 2. Doxorubicin release from analogs 3 and 4 under two different conditions.



Preparation of AuNPs. Gold nanoparticles (AuNPs) were prepared by two variations of the Wang method; method A with added AgNO_3 , and method B without added AgNO_3 .³⁷

Method A. AuNPs prepared by the Wang method with added AgNO_3 ³⁷ used a trace amount of silver nitrate to produce quasi-spherical AuNPs (Fig. S6). The citrate concentration was adjusted to produce nanoparticles with an average diameter of 41 nm, polydispersity index (PDI) of 0.212 and a Zeta potential of -26 ± 3 mV (Fig. S7a). PEGylated gold nanoparticles were prepared by treatment of a solution of gold nanoparticles with PEG methyl ether thiol; these had average

1
2
3 diameter of 49 nm, PDI of 0.317, and a Zeta potential of -16 ± 2 mV (Fig. S7b). Doxorubicin-
4
5 functionalized nanoparticles were prepared by treating a solution of nanoparticles prepared as
6
7 described above with doxorubicin analog **3** and mPEG thiol in CH₃OH, followed by repeated
8
9 centrifugation and resuspension to remove excess reagents. This gave soluble doxorubicin-
10
11 loaded nanoparticles **Au-3**. Incubation of **Au-3** at pH 4.6 in the presence of 10 mM glutathione at
12
13 37 °C for 72 h and analysis of the resulting solutions by HPLC showed a single peak which
14
15 matched that of doxorubicin. The area of the peak indicated that the drug loading of **3** was 0.78
16
17 mg analog per 1 mg of AuNP.
18
19

20
21 **Method B.** AuNPs were prepared by the Wang method without added AgNO₃.³⁷ The citrate
22
23 concentration was adjusted to produce approximately spherical nanoparticles with an average
24
25 diameter of 34.6 ± 0.1 nm as determined by TEM (Figures 4 and 5), and supported by dynamic
26
27 light scattering (Figure S8). The average diameters of the doxorubicin-functionalized
28
29 nanoparticles differed from the nonfunctionalized nanoparticles by less than 5% (Figures S9-
30
31 S20). The DLS of these and other nanoparticle preparations also showed signals for other size
32
33 particles, presumably due to weak aggregation of particles during storage. However, the
34
35 measured particle hydrodynamic diameter of the major population aligned with the size ranges
36
37 seen through TEM. Long-term sonication of these samples caused further destabilization and
38
39 aggregation of samples.
40
41
42
43
44
45
46
47
48
49
50
51
52
53
54
55
56
57
58
59
60

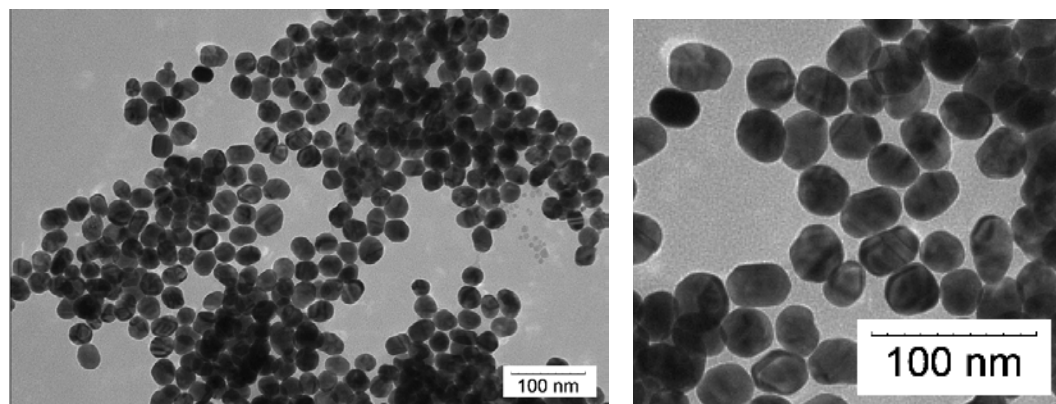


Figure 4. TEM images of naked AuNPs.

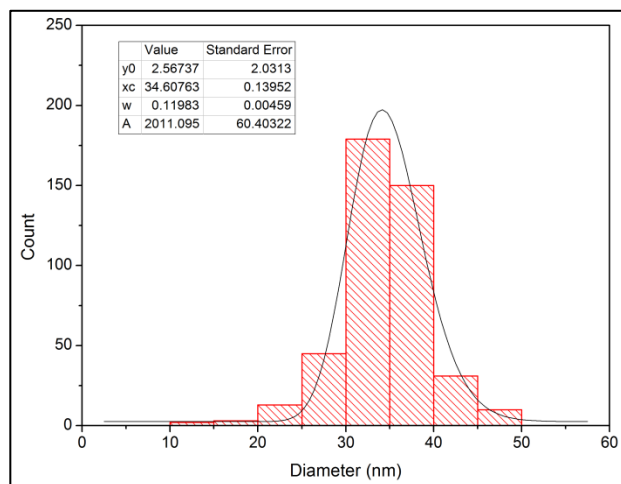


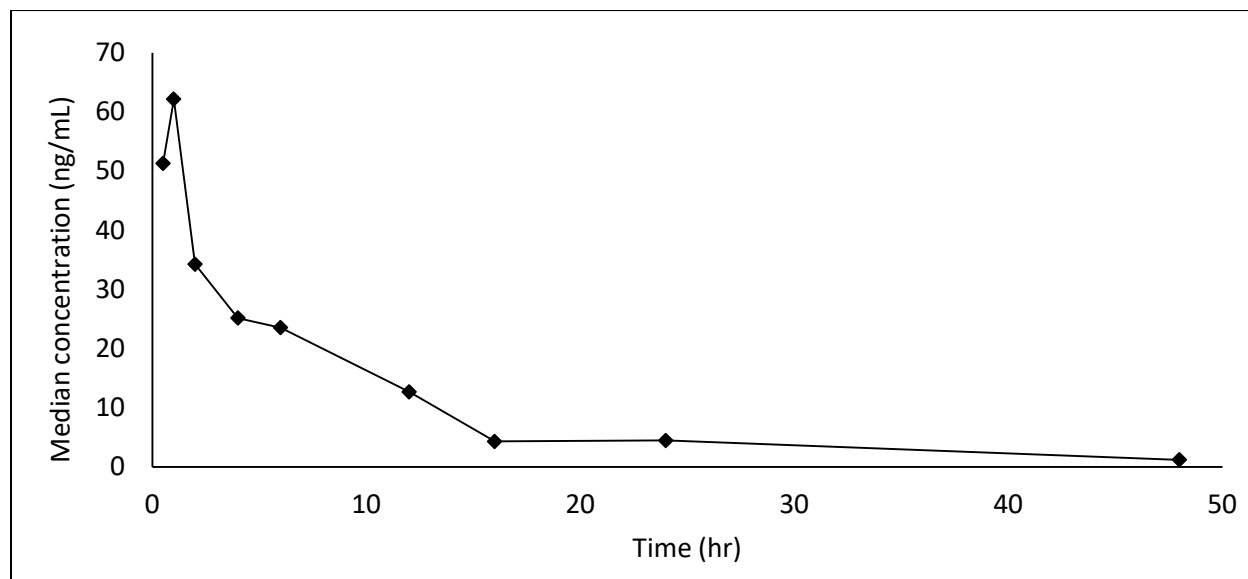
Figure 5. Image analysis of >400 AuNP, 5 nm bins fit to a LogNormal distribution (see equation in Supporting Information)

Drug loading and release of nanoparticles as a function of the concentration of PEG. Doxorubicin-functionalized nanoparticles were prepared by treating 50 mL of a solution of AuNP containing 2.5 mg AuNP with 6.67 mg of **3** in 100 mL CH₃OH and either 13.3 mg or 26.6 mg of PEG methyl ether thiol (mPEG thiol) in 1.0 mL water with stirring for 48 h, followed by repeated centrifugation and resuspension to remove excess reagents. The residue was dissolved in 1 mL water to give soluble doxorubicin-loaded nanoparticles **Au-3-1** (Figures S9 – S11) and **Au-3-2** (Figures S12 – S14) respectively, with gold contents of 1.05 and 1.70 mg as

1
2
3 determined by ICP-MS; the low recovery of AuNP reflects handling losses during the repeated
4 centrifugation and resuspension purification procedure. **Au-3-1** and **Au-3-2** were then incubated
5 with glutathione as described above for 72 h to ensure complete drug release, and the resulting
6 solutions were analyzed by HPLC. Both **Au-3-1** and **Au-3-2** gave a major peak which matched
7 that of doxorubicin. The areas of the peaks combined with ICP-MS data indicated that **Au-3-1**
8 had a loading of 0.018 mg per mg AuNP, while **Au-3-2** had a loading of 0.012 mg per mg AuNP.
9 This result indicates that the concentration of mPEG thiol affects drug loading, with the higher
10 concentration of mPEG thiol reducing drug loading.
11
12
13
14
15
16
17
18
19
20
21

22 **Drug loading and release of nanoparticles as a function of doxorubicin**
23 **concentration.** Doxorubicin-functionalized nanoparticles were prepared by treating a solution
24 of AuNP prepared as described above with a fixed concentration of mPEG thiol of 88.67 $\mu\text{g/mL}$
25 (17.7 μM) and concentrations of **3** of 6.67, 13.34 and 20 $\mu\text{g/mL}$ (8.87, 17.7, and 26.6 μM) in
26 CH_3OH , followed by centrifugation and resuspension to remove excess reagents. This gave
27 soluble doxorubicin-loaded nanoparticles **Au-3-1**, **Au-3-3** (Figures S15 – S17) and **Au-3-4**
28 (Figures S18 – S20) with gold contents of 1.05, 0.39 and 1.79 mg as determined by ICP-MS.
29 Samples of each of the three doxorubicin-loaded nanoparticles were incubated in the presence of
30 5 mM glutathione and analyzed as described above, and the resulting chromatograms of each
31 exhibited a major peak which matched that of doxorubicin. The area of the peak and the ICP-MS
32 data indicated that **Au-3-1** had a loading of 0.018 mg per mg AuNP, while **Au-3-3** had a loading
33 of 0.034 mg per mg AuNP and **Au-3-4** had a loading of 0.050 mg per mg AuNP. These data
34 indicated unsurprisingly that the doxorubicin loading increased as the initial concentration of
35 doxorubicin analog **3** increased.
36
37
38
39
40
41
42
43
44
45
46
47
48
49
50
51
52
53
54
55
56
57
58
59
60

1
2
3 **Pharmacokinetics of doxorubicin and Au-3 in mouse plasma.** Treatment of seventy-
4 two CD-1 mice with either doxorubicin hydrochloride at 6 mg/Kg or **Au-3** containing 6 mg/Kg
5 doxorubicin, followed by euthanasia in groups of 4 at ½, 1, 2, 4, 6, 12, 16, 24 and 48 hours post-
6 dose, was followed by analysis of blood plasma samples for doxorubicin by LC-MS/MS.
7
8 Doxorubicin concentration in plasma from the doxorubicin group started at 35 ng/mL and fell to
9 less than 5 ng/mL over 16 hours (Figure 6 and Tables S4 and S5). On the other hand the
10 doxorubicin concentration in plasma from the **Au-3** group started at 0.14 ng/mL and fell to
11 almost undetectable levels over 16 hours (Figure 7 and Tables S6 and S7). This experiment
12 indicated that almost all of the doxorubicin administered as the nanoparticle formulation **Au-3**
13 remained bound to the nanoparticle in mouse blood, and was not released into the plasma.
14
15
16
17
18
19
20
21
22
23
24
25



26
27
28
29
30
31
32
33
34
35
36
37
38
39
40
41
42
43
44
45 **Figure 6.** Median doxorubicin concentration in plasma from mice treated with 6 mg/kg doxorubicin.
46
47
48
49
50
51
52
53
54
55
56
57
58
59
60

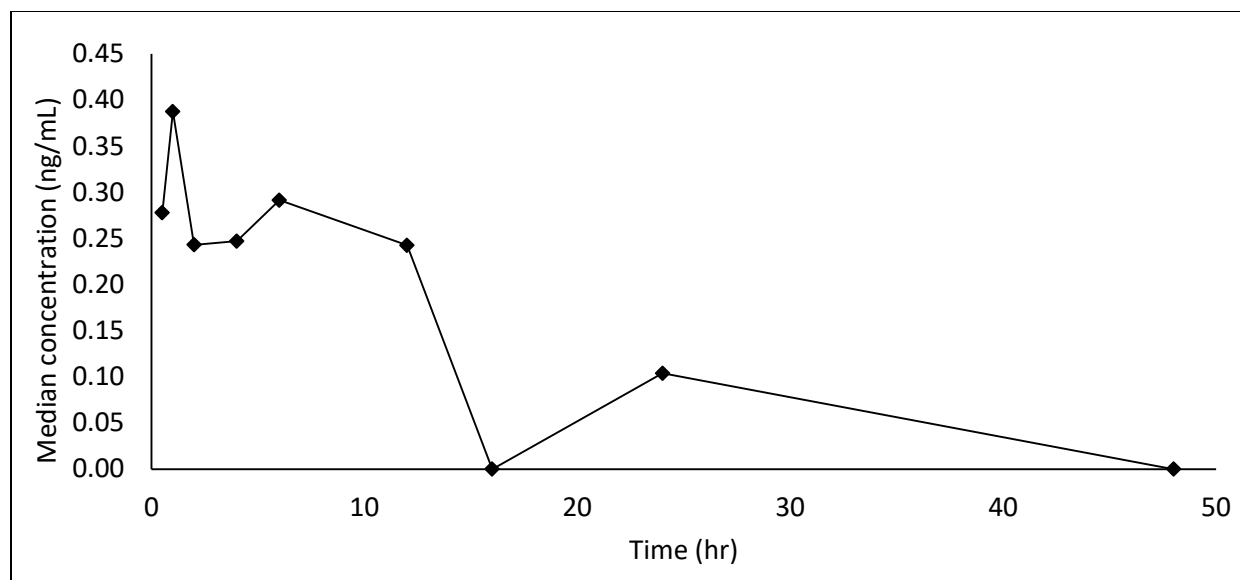


Figure 7. Median doxorubicin concentration in plasma from mice treated with 6 mg/kg doxorubicin as **Au-3**. Note the different concentration scale from Figure 4.

Safety of doxorubicin and Au-3 to mice. Forty-eight male, CD-1 mice were given a single IV dose of saline vehicle (dose group 1), 6 mg/kg doxorubicin hydrochloride (dose group 2) or 6 mg/kg doxorubicin as **Au-3** (dose group 3). The dose of doxorubicin was based on equivalent human doses³⁸ and previous experience of toxic effects that followed IV administration of doxorubicin to rodents.³⁹ The dose chosen was below that capable of causing the overt neurotoxicity previously reported yet within the possibility of dosages used for therapeutic purposes in people.

Neurobehavioral Assessment analysis. As part of the safety study, mice were evaluated for neurobehavioral endpoints as described in the Experimental Section using the endpoints of Table S8. Only the tail condition showed some variation between the treatment groups, but the proportions of abnormal tails were not significantly different between the groups at any of the time points (P-values > 0.05) (Table S9).

Effect of treatment on body weight. At baseline the groups of mice were balanced for weight, and each group showed moderate weight gain during the study. At 2 and 4 days of post-

dosing, the groups were not significantly different, but at 14 days, the least squares mean for group 3 (35.62 SE 0.40) was significantly greater than the least squares mean for group 1 (34.26 SE 0.39) (0.0488). Similarly, the least squares mean for group 3 (35.62 SE 0.40) was significantly greater than the least squares mean for group 2 (33.41 SE 0.40) (0.0008). Group 1 was not significantly different from group 2 (Figure 8). Least squares means (standard error) are presented in Table S10.

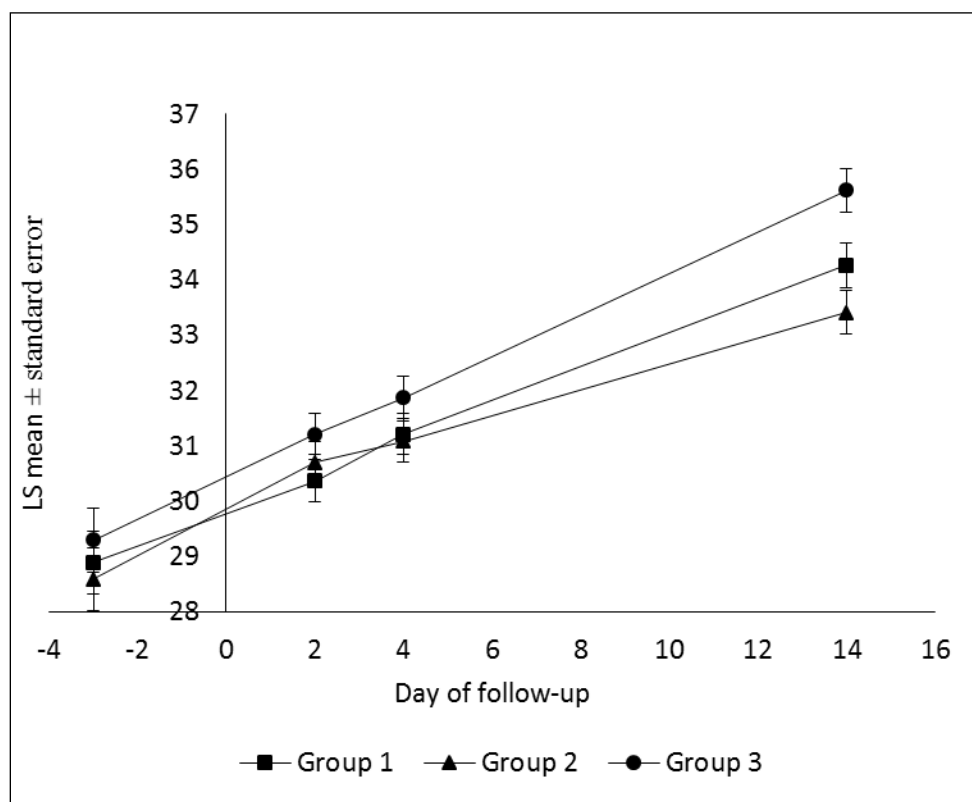


Figure 8. Effect of treatment on body weight in grams. Group 1 saline; group 2 doxorubicin.HCl; group 3 Au-3.

Clinical Pathology. Review of the chemistry panel and hematology panel showed that 4/4 mice given native doxorubicin (group 2) had significantly decreased reticulocyte counts 2 and 4 days after dosing (range of 2-33 compared to range of 201-340 in group 1 control mice). At 14 days post dosing 3 of 4 mice had counts above the range of the controls (414, 466, 745), with this

1
2
3 also providing significant difference from controls ($p < 0.05$). No such effects were noted with
4
5 the mice given **Au-3** (group 3, Figure S7).
6

7 **Histopathology.** Non-blinded histologic examination was performed on the following H&E-
8
9 stained sections of paraffin-embedded tissues: heart, lung, stomach, small intestine, large
10
11 intestine, liver, pancreas, kidney, adrenal, testes, spleen, thymus, skeletal muscle, vertebral bone
12
13 marrow, brain, spinal cord, and some dorsal root ganglions. Samples were obtained from
14
15 animals sacrificed on post-dosing days 2, 4 and 14. Histopathological lesions, viewed after
16
17 staining with hematoxylin and eosin, were restricted to the group of mice receiving conventional
18
19 doxorubicin by IV injection. On post-dosing day 2 there was marked erythroid hypoplasia and
20
21 reduced overall cellularity of the hematopoietic elements of the marrow, seen in 4/4 Group 2
22
23 mice. Myeloid cells were prominent, but whether this was due to hyperplasia or was relative due
24
25 to the erythroid hypoplasia could not be determined. On day 4 erythroid hypoplasia was still
26
27 evident in 3/4 mice, along with myeloid hyperplasia. By day 14 the bone marrow of the Group 2
28
29 animals had returned to normal. No changes in megakaryocytes was detected in the 2 or 4 day
30
31 Group 2 mice. The appearance of the bone marrow in Group 3 (6 mg/kg doxorubicin-AuNP)
32
33 was similar to that of Group 1 (vehicle control) at all stages. Occasional incidental background
34
35 changes in various tissues, of no significance, were seen in all Groups.
36
37
38
39
40
41
42
43

44 ■ DISCUSSION

45
46 The above data show that doxorubicin analog **3** is stable both in pH 7.4 and 4.6 buffer solutions
47
48 and that it binds well to AuNPs in the presence of mPEG thiol. The loading of **3** on AuNP can be
49
50 varied by adjusting the ratio of **3** and mPEG thiol, and the nanoparticle-bound forms of **3** all
51
52 release doxorubicin cleanly from the nanoparticles under reducing conditions. The highly
53
54
55
56
57
58
59
60

1
2
3 doxorubicin-loaded nanoparticle form **Au-3** was evaluated pharmacologically, and is stable in
4 mouse blood. Significantly lower plasma levels of doxorubicin were noted in plasma samples
5
6 from mice given **Au-3** when compared to those given conventional doxorubicin, suggesting that
7
8 its nanoparticle-bound form contributed to protection from pathological defects. Treatment of
9
10 mice with **Au-3** gave no histopathologically observable differences from mice treated with
11
12 saline, while mice treated with doxorubicin showed significant histopathologically observable
13
14 lesions. These results suggest that **Au-3** is has significantly reduced toxicity to normal cells as
15
16 compared with doxorubicin. Whether the nanoparticle formulation of doxorubicin, with its
17
18 longer half-life, would be effective in a clinical situation would require efficacy studies in
19
20 diseased subjects. However, since TNF is known to target AuNPs to tumors,³⁵ these results
21
22 suggest that linking of TNF to **Au-3** would provide a potent delivery vehicle for doxorubicin that
23
24 lacks some of the major side effects of this potent chemotherapeutic agent.
25
26
27
28
29
30
31
32

33 ■ EXPERIMENTAL SECTION

34
35 The following standard conditions apply unless other stated. All chemicals were purchased from
36
37 Sigma-Aldrich and used as received unless otherwise stated. Doxorubicin hydrochloride was
38
39 purchased from Wonda Science Inc, USA, amino-dPEGTM₄ acid was obtained from
40
41 QuantBioDesign, Ltd., Powell, OH, and methoxypolyethylene glycol thiol (5 kDa) was
42
43 obtained from Creative PEGworks. All glassware was oven-dried and all reactions were
44
45 conducted under nitrogen. Dichloromethane (CH₂Cl₂) was distilled from CaCl₂, tetrahydrofuran
46
47 (THF) was distilled from CaH₂, anhydrous methanol (MeOH) was purchased directly from
48
49 Sigma-Aldrich. Thin layer chromatography (TLC) was used to monitor the reaction progress on
50
51 silica gel UV₂₅₄. Purification was achieved either by column chromatography over silica gel 60
52
53
54
55
56
57
58
59
60

(220–240 mesh), or preparative thin layer chromatography (PTLC) on glass-backed plates coated with silica UV₂₅₄. HPLC was performed on Shimadzu SCL-10AVP system using a column purchased from Phenomenex (Luna 5 μ C18 (2) 25 x 4.6 mm). ¹H and ¹³C NMR spectra were obtained on an Agilent U4-DD2 spectrometer at 400 MHz for ¹H and 100 MHz for ¹³C or a Bruker Avance II spectrometer at 500 MHz for ¹H and 125 MHz for ¹³C. All chemical shifts were referenced to the solvent peaks of CDCl₃ (7.26 ppm for ¹H and 77.16 ppm for ¹³C) unless otherwise stated. An Agilent 6220 accurate-mass TOF LC/MS instrument was used to obtain high-resolution mass spectra of pure compounds, an Agilent 6470 Triple Quad LC-MS/MS was used for analysis of samples from biological media at the Virginia Tech Toxicology Diagnostic Laboratory, and an ICP-MS (Thermo Electron X-Series) following APHA Standard Method 3125-B (American Public Health Association et al., 1998) was used for analysis of concentrations of gold content in the Civil and Environmental Engineering Department at Virginia Tech. Specific protocols for animal experiments were reviewed and approved by Virginia Tech's Institutional Animal Care and Use Committee (IACUC).

4-(Acetylthio)benzoic acid (9). A 25 mL round bottom flask was oven-dried, cooled to room temperature and charged with a magnetic stirring bar, 4-mercaptobenzoic acid **8** (154 mg, 1.0 mmol), and a rubber septum. Dry CH₂Cl₂ (5 mL) was added via syringe to dissolve the solid and followed by adding C₅H₅N (0.323 mL, 4.0 mmol). An ice bath was used to cool the solution to 0 °C, followed by vigorous stirring for 5 min. After the solid was dissolved completely, Ac₂O (0.1 mL, 1.06 mmol) was added over a period of 10 min via syringe. The resulting mixture was warmed to room temperature and stirred for 6 h under nitrogen (balloon). The reaction was diluted with EtOAc (100 mL), washed with 0.6 M HCl solution (2 x 10 mL), brine (2 x 20 mL), and dried with anhydrous Na₂SO₄. After evaporating the solvent by rotary evaporation (25 °C), a

1
2
3 white crude product was obtained and purified by PTLC (eluted with CHCl₃:MeOH, 13:1) to
4
5 yield **9** (192 mg, 0.98 mmol) as a white powder in a yield of 98%. ¹H NMR (CD₃OD, 500 MHz,
6
7 δ): δ 8.05 (dd, *J* = 8.5, 2 Hz, 2H), 7.54 (dd, *J* = 8.5, 2 Hz, 2H), 2.44 (s, 3H); ¹³C NMR (126
8
9 MHz, δ): δ 194.2, 169.1, 135.2, 135.0, 132.8, 131.2, 30.3; HRESIMS: (*m/z*) [M – H][–] calcd for
10
11 C₉H₇O₃S, 195.0121; found 195.0124.

12
13
14 **S-(4-(hydroxymethyl)phenyl) ethanethioate (10)**. A 10 mL round bottom flask was oven-
15
16 dried, cooled to room temperature and charged with a magnetic stirring bar, compound **9** (192
17
18 mg, 0.98 mmol), and a rubber septum. The flask was evacuated for 5 min and flushed with
19
20 nitrogen. Dry THF (3 mL) was added to dissolve the solid. An ice-salt bath was used to cool the
21
22 solution to –10 °C, followed by vigorous stirring for 5 min. A solution of (CH₃)₂S•BH₃ in THF
23
24 (1.0 mL, 2.0 mmol) was added over a period of 10 min via syringe. The resulting mixture was
25
26 warmed to room temperature and stirred for 4 h under nitrogen (balloon). H₂O (2 mL) was added
27
28 to remove unreacted (CH₃)₂S•BH₃, the solution was diluted with EtOAc (100 mL), washed with
29
30 brine (2 x 20 mL), and dried with anhydrous Na₂SO₄. After evaporating the solvent by rotary
31
32 evaporation (30 °C), a liquid crude product was obtained, which was purified by PTLC (eluted
33
34 with CHCl₃:MeOH, 15:1) to yield **10** (151 mg, 0.83 mmol) as a colorless liquid in a yield of
35
36 85%. ¹H NMR (CD₃OD, 500 MHz, δ): δ 7.36 (m, 4H), 4.60 (s, 2H), 2.34 (s, 3H); ¹³C NMR (126
37
38 MHz, δ): 194.5, 143.2, 134.2, 127.2, 126.6, 63.2, 28.6; HRESIMS: (*m/z*) [M + H]⁺ calcd for
39
40 C₉H₁₁O₂S⁺, 183.0474; found 183.0466.

41
42
43 **S-4-(((4-nitrophenoxy)carbonyloxy)methyl)-phenyl ethanethioate (11)**. A 50 mL
44
45 round bottom flask was oven-dried, cooled to room temperature and charged with a magnetic
46
47 stirring bar, compound **10** (151 mg, 0.83 mmol), and a rubber septum. Dry CH₂Cl₂ (10 mL) was
48
49 added via syringe to dissolve the liquid followed by adding C₅H₅N (0.202 mL, 2.5 mmol). An ice
50
51
52
53
54
55
56
57
58
59
60

1
2
3 bath was used to cool the solution to 0 °C, followed by vigorous stirring for 5 min. A solution of
4
5 4-nitrophenyl chloroformate (168 mg, 0.83 mmol) in 5 mL CH₂Cl₂ was added over a period of 10
6
7 min via syringe. The resulting mixture was warmed to room temperature and stirred for 4 h
8
9 under nitrogen (balloon). The reaction was diluted with EtOAc (100 mL), washed with saturated
10
11 NaHCO₃ solution (2 x 10 mL), H₂O (2 x 10 mL) and brine (2 x 10 mL), and dried with
12
13 anhydrous Na₂SO₄. The solid crude obtained after evaporation was purified by column
14
15 chromatography (silica gel, 100 g, eluted with hexane:CH₂Cl₂, 5:1) to yield **11** (253 mg, 0.73
16
17 mmol) as a white powder in a yield of 88%. ¹H NMR (CDCl₃, 500 MHz, δ): 8.27 (dd, *J* = 9, 2
18
19 Hz, 2H), 7.47 (m, 4H), 7.38 (dd, *J* = 9, 2 Hz, 2H), 5.31 (s, 2H), 2.44 (s, 3H); ¹³C NMR (126
20
21 MHz, δ): 193.7, 155.5, 152.5, 145.5, 135.6, 134.8, 129.3, 129.0, 125.4, 121.9, 70.2, 30.4;
22
23 HRESIMS (*m/z*) [M + NH₄]⁺ calcd for C₁₆H₁₇N₂O₆S⁺, 365.0807; found 365.0795.
24
25
26
27

28
29 **Doxorubicin Analog 3: S-(4-((((2S,3S,4S,6R)-3-hydroxy-2-methyl-6-(((1S,3S)-**
30
31 **3,5,12-trihydroxy-3-(2-hydroxyacetyl)-10-methoxy-6,11-dioxo-1,2,3,4,6,11-**
32
33 **hexahydrotetracen-1-yl)oxy)tetrahydro-2H-pyran-4yl)carbamoyl)oxy**
34
35 **methyl)phenyl) ethanethioate.**

36
37 A 10 mL round bottom flask was oven-dried, cooled to room
38
39 temperature and charged with a magnetic stirring bar, doxorubicin hydrochloride (20 mg, 0.0345
40
41 mmol), compound **11** (20 mg, 0.0576 mmol), and a rubber septum. Anhydrous DMF (5 mL) was
42
43 added by syringe to dissolve the solids. An ice bath was used to cool the solution to 0 °C,
44
45 followed by vigorous stirring for 5 min. Then Et₃N (0.013 mL, 0.0988 mmol) was added to the
46
47 solution over a period of 5 min via syringe. The resulting mixture was warmed to room
48
49 temperature and stirred for 2 h under nitrogen (balloon). The reaction was diluted with EtOAc
50
51 (30 mL), washed with 0.6 M HCl solution (2 x 5 mL), saturated sodium NaHCO₃ (2 x 5 mL),
52
53 brine (2 x 10 mL), and dried with anhydrous Na₂SO₄. The crude product was purified by PTLC
54
55
56
57
58
59
60

(eluted with CHCl₃:MeOH, 13:1) to yield **3** (22.3 mg, 0.0297 mmol) as a red solid in a yield of 86%. ¹H NMR (CDCl₃, 500 MHz, δ): 13.95 (s, 1H, -OH), 13.21 (s, 1H, -OH), 8.02 (dd, *J* = 8.0, 1.1 Hz, 1H), 7.78 (t, *J* = 8.0 Hz, 1H), 7.39 (dd, *J* = 8.0, 1.1 Hz, 1H), 7.34 (m, 4H), 5.50 (d, *J* = 4.0 Hz, 1H), 5.27 (d, *J* = 3.5 Hz, 1H), 5.19 (d, *J* = 8.6 Hz, 1H, -OH), 5.04 (s, 2H), 4.75 (dd, *J* = 5.0, 2.0 Hz, 2H), 4.53 (s, 1H, -OH), 4.13 (q, *J* = 6.5 Hz, 1H), 4.07 (s, 3H), 3.86 (m, 1H), 3.66 (d, *J* = 5.6 Hz, 1H), 3.25 (dd, *J* = 18.8, 2.0 Hz, 1H), 3.02 (t, *J* = 5.0 Hz, 1H, -OH), 3.00 (d, *J* = 18.8 Hz, 1H), 2.39 (s, 3H), 2.32 (dt, *J* = 14.7, 2.0 Hz, 1H), 2.16 (dd, *J* = 14.7, 3.5 Hz, 1H), 2.05 (d, *J* = 7.5 Hz, 1H, -OH), 1.87 (dd, *J* = 13.2, 5.1 Hz, 1H), 1.77 (td, *J* = 13.2, 4.0 Hz, 1H), 1.25 (d, *J* = 6.5 Hz, 3H); ¹³C NMR (126 MHz, δ): 214.0, 194.0, 187.2, 186.8, 161.2, 156.3, 155.8, 155.5, 138.0, 135.9, 135.6, 134.7, 133.7, 133.6, 128.8, 127.8, 121.0, 120.0, 118.6, 111.7, 111.6, 100.9, 69.8, 69.7, 67.4, 66.2, 65.7, 56.8, 47.2, 35.8, 34.1, 30.4, 30.3 17.0; HRESIMS: (*m/z*) [M + Na]⁺ calcd for C₃₇H₃₇NO₁₄SNa⁺, 774.1832: found 774.1840.

Stability studies of analog 3. Calibration curves for free doxorubicin and analog **3** were constructed as described in the SI (Fig. S1). Analog **3** was then dissolved in a 1:3 mixture of methanol and PBS buffer (pH 7.4) or sodium acetate buffer (pH 4.6); methanol was used to increase the solubility of the analog. Both solutions were stirring vigorously at 37 °C. Aliquots were taken at various time points over a 72 h range, and their concentrations were determined by quantitative HPLC analysis on a Phenomenex Luna 5μ C18 column, 25 x 4.6 mm, with gradient elution from 30% CH₃CN:70% H₂O at 0 min to 100% CH₃CN:0% H₂O at 30 min and detection by UV lamp at 253 nm. The concentration of analog at each time point was calculated from the calibration curves (Fig. S2).

Preparation of monodisperse spherical AuNPs. A 25 mL round bottom flask was charged with 1.5 mL sodium citrate aqueous solution (1 wt %) and a magnetic stirring bar.

1
2
3 Aqueous HAuCl₄ (5.0 mL containing 12.5 mg Au as) was added, and H₂O (6.0 mL) was added
4
5 to bring the volume of the solution to 12.5 mL. This mixture was incubated for 5 min before
6
7 rapid addition to 237.5 mL of boiling H₂O in a 500 mL two-necked round bottom flask with
8
9 vigorous stirring. The color of the reaction solution changed quickly from colorless, grayish blue
10
11 to purple and then to ruby red within 1 min. The reaction solution was refluxed for 30 min under
12
13 stirring to promote formation of uniform quasi-spherical AuNPs.
14
15

16
17 Excess sodium citrate and other small molecules were removed by dialysis using dialysis
18
19 tubing with a MW cutoff of 3,500 Da and immersing it in 4 L water with vigorous stirring. The
20
21 water was changed every 2 hours over an 8 hour period and the resulting solution (250 mL) was
22
23 used for the following steps.
24
25

26 **Transmission Electron Microscopy.** Aliquots of 0.01 mL of the AuNP suspensions were
27
28 deposited on carbon-coated 200-mesh copper grids. The aqueous droplet was left to dry in
29
30 ambient conditions, typically for ~1 hour. Grids were imaged using a Philips EM420 electron
31
32 microscope with an accelerating voltage of 120 kV to enhance the contrast of the electron-dense
33
34 gold. Enough frames were collected to capture at least 400 particles per replicate. Nanoparticle
35
36 diameter (d) was estimated using the formula $d = A/\pi$, where A is the cross-sectional area of a
37
38 particle measured using ImageJ software.
39
40

41
42 **Dynamic Light Scattering.** Aliquots of 0.1 mL of each suspension were diluted to 1 mL with
43
44 DI H₂O. The hydrodynamic diameter (HD) and PDI were measured in polystyrene cuvettes
45
46 under 25 °C after an equilibration time of 120 seconds using a Malvern Zetasizer NanoZS.
47
48

49 **Synthesis of Doxorubicin Loaded AuNPs.** A 50 mL aqueous solution of AuNPs
50
51 containing 2.5 mg AuNP as described above, a 100 mL solution of 1 mg doxorubicin analog **3** in
52
53 CH₃OH, and a 1 mL aqueous solution of either 13.3 mg or 26.6 mg mPEG thiol (5 kDa) were
54
55
56
57
58
59
60

1
2
3 mixed and stirred for 48 h at room temperature. Unbound drugs and mPEG thiol were removed
4
5 by centrifugation on an Eppendorf Centrifuge 5810 R with a rotor diameter of 10 cm at 14,000
6
7 rpm (10,956 x g) for 20 min at room temperature, pipetting of the supernatant and re-dispersal of
8
9 the nanoparticle pellet in water. This process was repeated three times to remove the unbound
10
11 material completely. The residue was dissolved in 1.0 mL water to make **Au-3-1** and **Au-3-2**
12
13 respectively. Repetition of this process with 2 mg of **3** and 13.3 mg mPEG thiol gave **Au-3-3**,
14
15 and with 3 mg of **3** and 13.3 mg mPEG thiol gave **Au-3-4**. Four batches of each sample were
16
17 prepared.
18
19

20
21 **ICP-MS of Doxorubicin Loaded AuNPs.** A 10 μL aliquot of a 1.0 mL solution of **Au-3-1**
22
23 and 25 μL aliquots of solutions of **Au-3-2**, **Au-3-3** and **Au-3-4** in 10 mL water were used to
24
25 determine the concentration of Au by ICP-MS. The results were 1054, 4256, 982, and 4473 ppb
26
27 respectively, corresponding to 0.53, 0.85, 0.196 and 0.895 mg Au in 500 μL .
28
29

30
31 **Drug Release Studies of Analogs 3-1 – 3-4 from AuNP.** A 500 μL portion of each of the
32
33 four AuNP solutions prepared above was mixed with 500 μL sodium acetate buffer containing
34
35 10 mM GSH, and the pH was adjusted to 4.6. The solution was stirred vigorously at 37 $^{\circ}\text{C}$ for 72
36
37 h. The solution was then centrifuged at a speed of 14,000 rpm for 20 min. The four different
38
39 supernatants were evaporated and dissolved in 450 μL MeCN and 50 μL 0.6 M HCl, and
40
41 aliquots (100 μL) of the solution were injected onto an HPLC column and analyzed by
42
43 quantitative HPLC. **Au-3-1**, **Au-3-2**, **Au-3-3** and **Au-3-4** each gave a single peak which matched
44
45 that of doxorubicin. The areas of the peaks were compared with those of the standard curve, and
46
47 corresponding to masses of 0.00192, 0.00208, 0.00132 and 0.00899 mg per injection,
48
49 corresponding to 0.0096, 0.0104, 0.0066 and 0.045 mg per sample. After adjustment for the
50
51 differing masses of nanoparticles in each sample, these loadings correspond to drug loadings of
52
53
54
55
56
57
58
59
60

1
2
3 0.018, 0.012, 0.034, and 0.050 mg doxorubicin per 1 mg of AuNP for **Au-3-1** to **Au-3-4**,
4
5 respectively.

6
7 **Synthesis of Doxorubicin Loaded AuNPs Au-3 for Biological Studies.** A 10 mL
8
9 aqueous solution of AuNPs containing 10 mg AuNPs, a 20 mL solution of 10 mg doxorubicin
10
11 analog **3** in CH₃OH, and a 3 mL aqueous solution of 30 mg mPEG thiol (5 kDa) were mixed and
12
13 stirred for 48 h at room temperature. Unbound drugs and mPEG-thiol were removed by
14
15 centrifugation on an Eppendorf Centrifuge 5810 R with rotor diameter of 10 cm at 14,000 rpm
16
17 (10,956 x g) for 20 min at room temperature followed by removal of the supernatant by pipette
18
19 and re-dispersal of the nanoparticle pellet in water. This process was repeated three times to
20
21 remove the unbound material completely. The residue was dissolved in 1 mL water to give a
22
23 solution designated **Au-3**. Incubation of **Au-3** at pH 4.6 in the presence of 10 mM glutathione at
24
25 37 °C for 72 h and analysis of the resulting solutions by HPLC showed a single peak which
26
27 matched that of doxorubicin. The area of the peak indicated that the drug loading of **3** was 0.78
28
29 mg analog per 1 mg of AuNP.
30
31
32
33

34
35 **Pharmacokinetics of Doxorubicin and Au-3 in Mouse Plasma.** Seventy-two male,
36
37 CD-1 mice (Envigo) were used for the pharmacokinetic study. All animals were group housed
38
39 on Diamond Dry Cellulose Bedding (Envigo), given a standard pelleted rat chow and water ad
40
41 libitum. Mice were randomly assigned to dose groups. Dose groups consisted of either 6 mg/kg
42
43 doxorubicin hydrochloride (dose group 2) or Au-3 containing 6 mg/kg doxorubicin (dose group
44
45 3). Animals were intravenously dosed at time 0, and 4 animals per group were sacrificed at ½, 1,
46
47 2, 4, 6, 12, 16, 24 and 48 hours post-dosing with euthanasia by intraperitoneal injection of 200
48
49 mg/kg of sodium pentobarbital. Up to 1 mL of whole blood was collected in heparinized
50
51 syringes from the inferior vena cava to obtain plasma for LC-MS/MS analysis. The samples were
52
53
54
55
56
57
58
59
60

1
2
3 transferred to Vacutainer[®] blood collection tubes with added lithium heparin and centrifuged to
4 separate the plasma. The plasma supernatant was removed and stored in Eppendorf tubes at -70
5 °C until analyses could be done. For analysis the samples were extracted with acetonitrile and the
6 top organic layer containing doxorubicin was evaporated to dryness and analyzed by LC-MS/MS
7 with a H₂O:CH₃CN solvent gradient containing 1% formic acid (Table S1). Doxorubicin
8 extracted from blood was compared with that extracted from buffer, using free doxorubicin as
9 the internal standard (Figure S6). Daunorubicin was used as internal standard.

10
11
12 **Determination of Pharmacokinetic Properties.** Pharmacokinetic calculations were based
13 on 3 plasma samples per time point. Inspection of the time course plot showed that data
14 followed an approximate one-compartment model for the doxorubicin group. Median plasma
15 concentrations were entered into PKSolver⁴⁰ for determination of elimination rate constant (kel),
16 apparent volume of distribution (Vd), clearance (Cl) and half-life (t_{1/2}). The maximal
17 concentration (C_{max}) and the time to C_{max} (T_{max}) were determined from observing the graph of
18 median plasma concentrations versus time. Concentrations for the Au-3 group were all below 1
19 ng/mL and appeared to show more random variation over time.

20
21
22 **Safety of Doxorubicin and Au-3 to Mice.** Forty-eight male, CD-1 mice (Envigo) were
23 used for the safety study and maintained as described above. Dose groups consisted of either a
24 saline vehicle (dose group 1), 6 mg/kg doxorubicin hydrochloride (dose group 2) or Au-3 6
25 mg/kg AuNPs (dose group 3). All solutions were given once by IV injection of 0.05 mL volume
26 into the lateral tail vein.

27
28
29 A baseline neurobehavioral assessment was performed prior to dosing (study day -3) and
30 then again on study days 2, 4 (n = 10/group/timepoints) and 14 (n = 8/group). Each assessment
31 consisted of clinical observations scored as normal/abnormal or yes/no (observational category is

1
2
3 present/absent) and a recording of body weight. Physiological endpoints (weight, body
4 temperature) and observational endpoints (general appearance, mobility, nervous system
5 functioning) were compared between vehicle-dosed and test-agent dosed mice. Mice (4/group)
6 were sacrificed by pentobarbital overdose at 2, 4 and 14 days and underwent examination for
7 detrimental effects as determined by clinical pathology and histopathology. The following tissues
8 were collected and immersion-fixed in 10% neutral buffered formalin: brain, heart, lung,
9 thymus, stomach, duodenum/pancreas, small intestine, large intestine, liver, kidney, adrenal
10 gland, spleen, testes, gastrocnemius muscle and lumbar spinal column. Sections of tail were also
11 collected from animals sacrificed on day 14. Lumbar spinal column and tail samples were
12 decalcified overnight in EDF[®] prior to all tissues being trimmed and analyzed by the
13 Histopathology Laboratory of the Veterinary Medical Teaching Hospital. There the samples
14 were dehydrated and cleared and embedded in Paraplast[®]. The samples were then sectioned at 5
15 μm thickness, stained with hematoxylin and eosin (H&E) for pathological examination by light
16 microscopy (Figure S7).

17
18
19 For clinical pathology, up to 1 mL of whole blood was collected using heparinized
20 syringes. Blood samples were transferred to two Microtainer[®] tubes, one with added lithium
21 heparin and one with K₂EDTA (up to 500 μL each). Samples were then analyzed by the Clinical
22 Pathology Laboratory of the Veterinary Medical Teaching Hospital for blood chemistry (Table
23 S9).

24
25
26 **Statistical Analysis of Behavior Data.** Categorical endpoints of the Neurobehavioral
27 Assessment investigated are listed in Table S6. Subsequently the proportion of abnormal tails
28 were compared between the groups at each time point using the Mantel-Haenszel Chi-Square.
29 For the continuous endpoint of body weight, the treatment groups were compared using mixed-

1
2
3 model analysis of variance (at baseline) and mixed-model analysis of covariance (with baseline
4 measurements as covariates) at each time point during follow up. All analyses controlled for
5
6 block as specified in the study design.
7
8
9

10 11 ■ ASSOCIATED CONTENT

12 13 14 Supporting Information

15
16 The Supporting Information is available free of charge on the ACS Publications website at
17
18 DOI:10.1021/acs.bioconjchem.7b00164y

19
20 Synthetic procedures for analogs **4** – **7**, ^1H and ^{13}C NMR spectra of all new compounds,
21
22 experimental description of bioanalytical methods, Tables S1 – S3, and Figures S1 – S25.
23
24
25

26 27 ■ AUTHOR INFORMATION

28 29 Corresponding Author

30
31 *D.G.I.K.: e-mail, dkingston@vt.edu; phone, +1 540-231-6570

32
33 Yongle Du and Long Xia contributed equally to this work.
34
35
36
37

38 39 Notes

40
41 The authors declare the following competing financial interests: D.G.I.K. holds stock options in
42
43 CytImmune Sciences, Inc., a company that is developing AuNP-based drug delivery systems.
44
45

46 47 ■ ACKNOWLEDGMENTS

48
49 This work was supported in part by a grant from the Virginia Tech Institute for Critical
50
51 Technology and Applied Science “A Nanotechnology Approach to Overcome the Barriers of
52
53 Cancer Drug Delivery.” The authors thank Peggy Brodie, Qingxi Su and Ming Wang for
54
55 determining the IC_{50} values of the analogs against the A2780 ovarian cancer cell line.
56
57
58
59
60

1
2
3 Drs. Bernard S. Jortner, Katie Boes, and Stephen Werre of the College of Veterinary Medicine at
4
5 Virginia Tech provided results for histopathology, clinical pathology, and statistics (including
6
7 pharmacokinetics), respectively. Jonathan Hinckley dosed the mice, did behavioral observations,
8
9 collected blood and tissue samples, and prepared the formalin-fixed tissue for histopathological
10
11 processing and staining.
12
13

14 ■ REFERENCES

- 15
16
17
18 (1) Arcamone, F., Cassindelli, G., Fantini, G., Orezzi, P., Pol, C., and Spalla, C. (1969)
19 Adriamycin, 14-hydroxydaunomycin, a new antitumor antibiotic from *S. peucetius* var.
20 *caesius*. *Biotechnol. Bioeng.* 11, 1101-1110.
21
22 (2) Arcamone, F.-M., Gaetani, M., Scotti, T., and Dimarco, A. (1961) Isolamento ed attivita
23 antitumorale di un antibiotico da *Streptomyces* sp. *Giorn. Microbiol.* 9, 83-90.
24
25 (3) Arcamone, F.-M. (2009) Fifty Years of Chemical Research at Farmitalia. *Chem. Eur. J.*
26 16, 7774.
27
28 (4) Arcamone, F.-M. (2012) Anthracyclines, in *Anticancer Agents from Natural Products*
29 (Cragg, G. M., Kingston, D. G. I., and Newman, D. J., Eds.) pp 383-406, CRC Press,
30 Boca Raton, FL.
31
32 (5) Lown, J. W. (1993) Discovery and development of anthracycline antitumour antibiotics.
33 *Chem. Soc. Rev.* 22, 165-176.
34
35 (6) Minotti, G., Menna, P., Salvatorelli, E., Cairo, G., and Gianni, L. (2004) Anthracyclines:
36 molecular advances and pharmacologic developments in antitumor activity and
37 cardiotoxicity. *Pharmacol. Rev.* 56, 185-229.
38
39 (7) Weiss, R. B. (1992) The anthracyclines: will we ever find a better doxorubicin? *Sem.*
40 *Oncol.* 19, 670-686.
41
42 (8) Hill, S. (2015), World Health Organization.
43
44 (9) Carvalho, F. S., Burgeiro, A., Garcia, R., Moreno, A. J., Carvalho, R. A., and Oliveira, P.
45 J. (2014) Doxorubicin-induced cardiotoxicity: From bioenergetic failure and cell death to
46 cardiomyopathy. *Med. Res. Rev.* 34, 106-135.
47
48 (10) Menna, P., Salvatorelli, E., Gianni, L., and Minotti, G. (2008) Anthracycline
49 cardiotoxicity. *Top. Curr. Chem.* 283, 21-44.
50
51 (11) Barenholz, Y. (2012) Doxil[®] — The first FDA-approved nano-drug: Lessons learned. *J.*
52 *Controlled Release* 160, 117-134.
53
54 (12) Batist, G., Barton, J., Chaikin, P., Swenson, C., and Welles, L. (2002) Myocet (liposome-
55 encapsulated doxorubicin citrate): a new approach in breast cancer therapy. *Expert Opin.*
56 *Pharmacother.* 3, 1739-1751.
57
58 (13) Chen, G., Li, D., Li, J., Cao, X., Wang, J., Shi, X., and Guo, R. (2015) Targeted
59 doxorubicin delivery to hepatocarcinoma cells by lactobionic acid-modified laponite
60 nanodisks. *New J. Chem.* 39, 2847-2855.
61
62 (14) Joniec, A., Sek, S., and Krysinski, P. (2016) Magnetoliposomes as potential carriers of
doxorubicin to tumours. *Chemistry* 22, 17715-17724.

- 1
- 2
- 3
- 4 (15) Liu, W., Wen, S., Shen, M., and Shi, X. (2014) Doxorubicin-loaded Poly(lactic-co-
- 5 glycolic acid) Hollow Microcapsules for Targeted Drug Delivery to Cancer Cells. *New J.*
- 6 *Chem.* 38, 3917-3924.
- 7 (16) Maeda, H. (2012) Macromolecular therapeutics in cancer treatment: The EPR effect and
- 8 beyond. *J. Controlled Release* 164, 138-144.
- 9 (17) Wilhelm, S., Tavares, A. J., Dai, Q., Ohta, S., Audet, J., Dvorak, H. F., and Chan, W. C.
- 10 W. (2016) Analysis of nanoparticle delivery to tumours. *Nat. Rev. Mater.* 1, 16014.
- 11 (18) Torrice, M. (2016) Does nanomedicine have a delivery problem? *Chem. Eng. News* 94
- 12 (25), 16-19.
- 13 (19) Kumar, A., Zhang, X., and Liang, X.-J. (2013) Gold nanoparticles: emerging paradigm
- 14 for targeted drug delivery system. *Biotechnol. Adv.* 31, 593-606.
- 15 (20) Mirza, A. Z., and Shamshad, H. (2011) Preparation and characterization of doxorubicin
- 16 functionalized gold nanoparticles. *Eur. J. Med. Chem* 346, 1857-1860.
- 17 (21) Chaudhary, A., Dwivedi, C., Gupta, A., and Nandi, C. K. (2015) One pot synthesis of
- 18 doxorubicin loaded gold nanoparticles for sustained drug release. *RSC Adv.* 5, 97330-
- 19 97334.
- 20 (22) Khandekar, S. V., Kulkarni, M. G., and Devarajan, P. V. (2014) Polyaspartic acid
- 21 functionalized gold nanoparticles for tumor targeted doxorubicin delivery. *J. Biomed.*
- 22 *Nanotechnol.* 10, 143-153.
- 23 (23) Alexander, C. M., Hamner, K. L., Maye, M. M., and Dabrowiak, J. C. (2014)
- 24 Multifunctional DNA-gold nanoparticles for targeted doxorubicin delivery. *Bioconjugate*
- 25 *Chem.* 25, 1261-1271.
- 26 (24) Zhang, Z.-M., Gao, P.-C., Wang, Z.-F., Sun, B.-W., and Jiang, Y. (2015) DNA-caged
- 27 gold nanoparticles for controlled release of doxorubicin triggered by a DNA enzyme and
- 28 pH. *Chem. Commun.* 51, 12996-12299.
- 29 (25) Spadavecchia, J., Movia, D., Moore, C., Maguire, C. M., Moustou, H., Casale, S.,
- 30 Volkov, Y., and Prina-Mello, A. (2016) Targeted polyethylene glycol gold nanoparticles
- 31 for the treatment of pancreatic cancer: from synthesis to proof-of-concept in vitro studies.
- 32 *Int. J. Nanomed.* 11, 791-822.
- 33 (26) Swiech, O. A., Opuchlik, L. J., Wojciuk, G., Stepkowski, T. M., Kruszewski, M., and
- 34 Bilewicz, R. (2016) Doxorubicin carriers based on Au nanoparticles - effect of shape and
- 35 gold-drug linker on the carrier toxicity and therapeutic performance. *RSC Adv.* 6, 31960-
- 36 31967.
- 37 (27) Asadishad, B., Vossoughi, M., and Alemzadeh, I. (2010) Folate-receptor-targeted
- 38 delivery of doxorubicin using polyethylene glycol-functionalized gold nanoparticles. *Ind.*
- 39 *Eng. Chem. Res.* 49, 1958-1963.
- 40 (28) Cheng, J., Gu, Y.-J., Cheng, S. H., and Wong, W.-T. (2013) Surface functionalized gold
- 41 nanoparticles for drug delivery. *J. Biomed. Nanotech.* 9, 1362-1369.
- 42 (29) Gu, Y.-J., Cheng, J., Man, C. W.-Y., Wong, W.-T., and Cheng, S. H. (2012) Gold-
- 43 doxorubicin nanoconjugates for overcoming multidrug resistance. *Nanomedicine:*
- 44 *Nanotechnology, Biology and Medicine* 8, 204-211.
- 45 (30) Aryal, S., Grailer, J. J., Pilla, S., Steeber, D. A., and Gong, S. (2009) Doxorubicin
- 46 conjugated gold nanoparticles as water-soluble and pH-responsive anticancer drug
- 47 nanocarriers. *J. Mater. Chem.* 19, 7879-7884.
- 48
- 49
- 50
- 51
- 52
- 53
- 54
- 55
- 56
- 57
- 58
- 59
- 60

- 1
2
3 (31) Prabakaran, M., Grailer, J. J., Pilla, S., Steeber, D. A., and Gong, S. (2009) Gold
4 nanoparticles with a monolayer of doxorubicin-conjugated amphiphilic block copolymer
5 for tumor-targeted drug delivery. *Biomaterials* 30, 6065-6075.
6
7 (32) Zhang, X., Chibli, H., Mielke, R., and Nadeau, J. (2011) Ultrasmall gold-doxorubicin
8 conjugates rapidly kill apoptosis-resistant cancer cells. *Bioconjugate Chem.* 22, 235-243.
9
10 (33) Gautier, J., Allard-Vannier, E., Munnier, E., Souce, M., and Chourpa, I. (2013) Recent
11 advances in theranostic nanocarriers of doxorubicin based on iron oxide and gold
12 nanoparticles. *J. Controlled Release* 169, 48-61.
13
14 (34) Bhamidipati, M., and Fabris, L. (2017) Multiparametric Assessment of Gold
15 Nanoparticle Cytotoxicity in Cancerous and Healthy Cells: The Role of Size, Shape, and
16 Surface Chemistry. *Bioconjug Chem* 28, 449-460.
17
18 (35) Paciotti, G. F., Zhao, J., Cao, S., Brodie, P. J., Tamarkin, L., Huhta, M., Myer, L. D.,
19 Friedman, J., and Kingston, D. G. I. (2016) Synthesis and evaluation of paclitaxel-loaded
20 gold nanoparticles for tumor-targeted drug delivery. *Bioconjugate Chem.* 27, 2646-2657.
21
22 (36) Janssen, M. J. H., Crommelin, D. J. A., Storm, G., and Hulshoff, A. (1985) Doxorubicin
23 decomposition on storage. Effect of pH, type of buffer and liposome encapsulation. *Int. J.*
24 *Pharmaceut.* 23, 1-11.
25
26 (37) Xia, H., Bai, S., Hartmann, J. r., and Wang, D. (2009) Synthesis of monodisperse quasi-
27 spherical gold nanoparticles in water via silver (I)-assisted citrate reduction. *Langmuir*
28 26, 3585-3589.
29
30 (38) Facts&Comparisons (2016) *Drug Facts and Comparisons 2016*, Facts and Comparisons,
31 St. Louis, MO.
32
33 (39) Cho, E. S., Spencer, P. S., Jortner, B. S., and Schaumburg, H. H. (1980) A single
34 intravenous injection of doxorubicin (Adriamycin[®]) induces sensory neuropathy in
35 rats. *NeuroToxicology* 1, 583-591.
36
37 (40) Zhang, Y., Huo, M., Zhou, J., and Xie, S. (2010) PKSolver: An add-in program for
38 pharmacokinetic and pharmacodynamic data analysis in Microsoft Excel. *Comp. Meth.*
39 *Prog. Biomed.* 99, 306-314.
40
41
42
43
44
45
46
47
48
49
50
51
52
53
54
55
56
57
58
59
60

Graphic for Abstract